

**4*f* hybridization effect on the magnetism of Nd<sub>2</sub>PdSi<sub>3</sub>**K. Mukherjee,<sup>\*</sup> Tathamay Basu, Kartik K. Iyer, and E. V. Sampathkumaran<sup>†</sup>*Tata Institute of Fundamental Research, Homi Bhabha Road, Colaba, Mumbai 400005, India*

(Received 21 July 2011; revised manuscript received 24 October 2011; published 14 November 2011)

Among the members of the series  $R_2\text{PdSi}_3$  ( $R$  = rare earth), the magnetic behavior of the Nd compound is interesting in some respects. This compound is considered to order ferromagnetically ( $<16$  K), unlike other members of this series, which order antiferromagnetically. In addition, the magnetic ordering temperature ( $T_o$ ) is significantly enhanced with respect to the de Gennes–scaled value. To understand the magnetism of this compound better, we have investigated the magnetic behavior in detail (and under external pressure) and examined its solid solutions based on substitutions at Nd and at Si sites, viz., on the series,  $\text{Nd}_{2-x}(\text{Y, La})_x\text{PdSi}_{3-y}\text{Ge}_y$  ( $x, y = 0.2, 0.4, 0.8, \text{ and } 1.2$ ) by bulk measurements. The results overall establish that  $\text{Nd}_2\text{PdSi}_3$  orders ferromagnetically below 16 K but an antiferromagnetic (AFM) component seems to set in at very low temperatures. However, there is significant suppression of  $T_o$  for Y and Ge substitutions compared to the La substitution for a given magnitude of unit cell volume change, qualitatively correlating with the separation between the layers of Nd and Pd-Si(Ge). On the basis of this observation, we conclude that 4*f*(Nd) hybridization plays a major role on the magnetism of the former solid solutions. To our knowledge, this work serves as a rare demonstration of the 4*f* hybridization effects on the magnetism of a Nd-based intermetallic compound.

DOI: [10.1103/PhysRevB.84.184415](https://doi.org/10.1103/PhysRevB.84.184415)

PACS number(s): 75.40.Cx, 71.20.Eh, 71.27.+a

**I. INTRODUCTION**

The 4*f* orbital is gradually localized as the 4*f* occupation number is increased for rare earth ( $R$ ). The investigation of the consequences of partial extension of the 4*f* orbital on the solid state properties of  $R$  intermetallics has been at the center of modern condensed matter physics research. Studies demonstrating 4*f* hybridization effects have been to a large extent restricted to Ce compounds and to a much lesser extent to Pr compounds,<sup>1</sup> but little detailed work exists in the literature for Nd compounds, barring some photoemission studies.<sup>2</sup> It is therefore of interest to focus investigations on Nd-based compounds.

In this paper, we bring out interesting 4*f* hybridization effects on the magnetism of the compound  $\text{Nd}_2\text{PdSi}_3$ , belonging to a  $\text{AlB}_2$ -derived ternary family<sup>3</sup> (hexagonal structure, space group  $P6/mmm$ ) with many exotic properties.<sup>4-21</sup> This ternary derivative arises out of ordered replacement of a B site by Pd and Si ions, resulting in two chemical environments for  $R$  ions. The unit cell is doubled within the basal plane with respect to the  $\text{AlB}_2$  unit cell. The Pd and Si atoms form two-dimensional hexagonal rings, and these layers are separated by  $R$  ions, as described in Ref. 4. This compound appears to be an interesting one in this family in the following respects. It is generally believed that this compound orders ferromagnetically<sup>3,7,21</sup> with weak frequency-dependent alternating current (AC) susceptibility  $\chi$  features below  $T_o$ ,<sup>15</sup> whereas in many other members of this series there is a paramagnetic–AFM transition followed by spin-glass-like features with lowering of the temperature. In addition, the observed magnetic ordering temperature ( $T_o = 16$  K) is about seven times larger than that expected on the basis of de Gennes scaling and only marginally lower than that observed<sup>5</sup> for  $\text{Gd}_2\text{PdSi}_3$  ( $T_N = 21$  K). Therefore, to understand this compound better, a detailed study involving magnetization ( $M$ ), heat capacity ( $C$ ), and electrical resistivity ( $\rho$ ) measurements was carried out. The same investigations were carried out on its solid solutions, based on substitutions at the Nd site or at the Si site, viz., on the

series  $\text{Nd}_{2-x}(\text{Y, La})_x\text{PdSi}_{3-y}\text{Ge}_y$  ( $x, y = 0.2, 0.4, 0.8, \text{ and } 1.2$ ), to shed more light on the behavior of Nd-4*f* in this chemical environment. In addition, high-pressure magnetization studies on the parent compound were carried out. The results, apart from revealing the complex nature of the magnetism of this compound, bring out the 4*f* hybridization effect on the magnetism of Nd.

**II. EXPERIMENTAL DETAILS**

Polycrystalline alloys of the solid solutions  $\text{Nd}_{2-x}(\text{Y, La})_x\text{PdSi}_{3-y}\text{Ge}_y$  ( $x, y = 0.2, 0.4, 0.8, \text{ and } 1.2$ ) were prepared by arc-melting stoichiometric amounts of respective high-purity elements in an atmosphere of argon and were subsequently homogenized by vacuum annealing in sealed quartz tube at 750 °C for a week. X-ray diffraction studies established that all specimens are single phase (Fig. 1) within the detection limit ( $<2\%$ ) of this technique and form in the proper structure. A comparison of the x-ray diffraction patterns of the parent and doped compounds (Fig. 1 inset) reveals a gradual shift of diffraction lines to the higher-angle side for the Y series and to the lower-angle side for the La/Ge series, thereby establishing that the dopants go to respective sites. The lattice parameters of the compound are listed in Table I.

The direct current (DC) magnetization  $M$  in the temperature  $T$  range of 1.8–300 K for all specimens was carried out with the help of a commercial superconducting quantum interference device (SQUID, Quantum Design). The AC susceptibility studies were also carried at selected frequencies. We performed heat capacity measurements employing a physical property measurements system (PPMS, Quantum Design) as a function of  $T$  in the range 1.8–100 K. The  $\rho$  measurements by a standard four-probe method, in the absence/presence of magnetic fields ( $H \leq 100$  kOe,  $T = 1.8$ –300 K), were performed with the same PPMS. A conducting silver paint was used for making electrical contacts of the leads with the samples. Further  $M$  measurements were carried out employing a commercial cell (Easy-Laboratory Technologies) in a hydrostatic pressure

TABLE I. The lattice constants ( $a$ ,  $c \pm 0.004 \text{ \AA}$ ), unit cell volume ( $V$ ), and magnetic ordering temperature ( $T_o \pm 0.5 \text{ K}$ ) for the alloys  $\text{Nd}_{2-x}(\text{Y, La})_x\text{PdSi}_{3-y}\text{Ge}_y$ .

| $x, y$              | $a$ ( $\text{\AA}$ ) | $c$ ( $\text{\AA}$ ) | $V$ ( $\text{\AA}^3$ ) | $T_o$ (K) |
|---------------------|----------------------|----------------------|------------------------|-----------|
| 0.0                 | 8.216                | 8.414                | 491.9                  | 15.5      |
| $\text{Y}_x = 0.2$  | 8.202                | 8.394                | 489.1                  | 13.4      |
| 0.4                 | 8.187                | 8.348                | 484.5                  | 10.0      |
| 0.8                 | 8.164                | 8.311                | 479.8                  | 5.2       |
| 1.2                 | 8.147                | 8.227                | 472.9                  | 2.9       |
| $\text{La}_x = 0.2$ | 8.228                | 8.443                | 495.1                  | 14.3      |
| 0.4                 | 8.229                | 8.479                | 497.3                  | 13.0      |
| 0.8                 | 8.252                | 8.545                | 503.9                  | 9.9       |
| 1.2                 | 8.273                | 8.607                | 510.2                  | 5.9       |
| $\text{Ge}_y = 0.2$ | 8.222                | 8.414                | 492.6                  | 13.0      |
| 0.4                 | 8.235                | 8.412                | 494.1                  | 12.5      |
| 0.8                 | 8.274                | 8.405                | 498.2                  | 10.7      |
| 1.2                 | 8.284                | 8.388                | 499.7                  | 7.5       |

medium ( $\leq 10$  kbar at 4.2 K) of Daphne oil with the help of the previously mentioned SQUID magnetometer. Unless stated otherwise, all measurements were done under zero field-cooled (ZFC) conditions of the specimens.

### III. RESULTS AND DISCUSSION

#### A. Complex nature of the magnetism of $\text{Nd}_2\text{PdSi}_3$

The inverse of magnetic susceptibility  $\chi$  measured in a magnetic field of 5 kOe is plotted as a function of temperature [Fig. 2(a)] and the Curie-Weiss fit [ $M/H = C/(T - \theta_p)$ , where  $C$  is a constant in this case] of the curve yields a Curie-Weiss temperature  $\theta_p$  of  $\sim 8$  K. The experimentally determined value of the effective moment of  $3.5 \mu_B/\text{Nd}^{3+}$  compares well with the free  $\text{Nd}^{3+}$  value of  $3.6 \mu_B$ , while the positive value of  $\theta_p$  points toward the dominance of ferromagnetic (FM) interaction. However, the value of  $\theta_p$  being less than  $T_o$  could indicate the presence of AFM correlations competing with FM interactions in the paramagnetic state, as observed for  $\text{Tb}_2\text{PdSi}_3$  in the same family.<sup>4</sup> The results on single crystals<sup>21</sup> revealed that the sign of  $\theta_p$  ( $\sim 9.5$  K) is positive for  $H//[001]$ , whereas it is negative (about  $-2.3$  K) along  $H//[100]$ , thereby offering evidence for the anisotropic nature of the magnetic interaction; interestingly, the difference between the magnitudes turns out to be nearly the same as the value of  $\theta_p$  in the polycrystalline sample.

The temperature dependence of DC magnetization under ZFC and field-cooled (FC) conditions at 100 Oe at low temperatures is shown in Fig. 2(b). The features attributable to magnetic ordering are clearly seen in the data near 15.5 K. A peak is observed just below  $T_o$  in the ZFC curve, which is followed by a drastic fall in the magnetization value, but the FC curve continuously rises with decreasing temperature. This fall in the ZFC curve is generally not characteristic of long-range ordered FM systems, in which the magnetization below  $T_o$  varies as the inverse of the demagnetization factor and is expected to be constant.<sup>22</sup> However, in the case of FM systems, we can see a bifurcation of ZFC-FC curves if the coercive field becomes larger than the externally applied field.

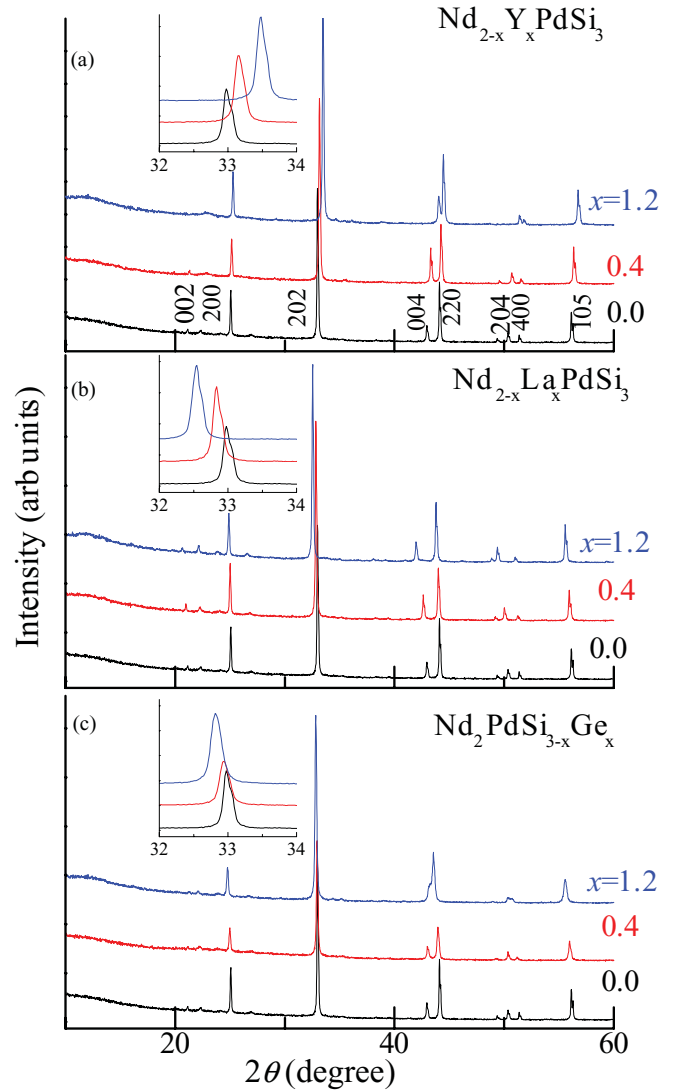


FIG. 1. (Color online) X-ray diffraction patterns ( $\text{Cu K}\alpha$ ) below  $2\theta = 60^\circ$  for the alloys,  $\text{Nd}_{2-x}(\text{Y, La})_x\text{PdSi}_{3-y}\text{Ge}_y$  (for selected compositions). The curves are shifted along the y-axis for clarity. Inset: The region around the main peaks is shown in an expanded form to show a gradual shift of diffraction lines with changing composition.

The coercive field in our sample diminishes with increasing temperature, e.g., 1.1 and 0.19 kOe at 1.8 and 5 K, respectively. Such a bifurcation is also sometimes observed<sup>23</sup> in anisotropic systems.

If we look at the  $M(H)$  curve at 1.8 K [Fig. 2(c)], a magnetic hysteresis (which is characteristic of FM systems) is observed and the magnetization does not saturate until high fields. The studies extended with a commercial vibration sample magnetometer (Quantum Design) to higher fields revealed that this trend persists until the highest field employed (160 kOe). Also, in Ref. 21, isothermal magnetization was reported up to 120 kOe and there is a weak variation for easy axis  $H//[001]$  until high fields. The nonsaturation tendency of magnetization is usually noted for systems with finite AFM correlations even at high fields at 1.8 K. The virgin curve at low fields is nearly flat, resulting in S-shaped curvature. With increasing temperature, this S-shaped curvature is gradually

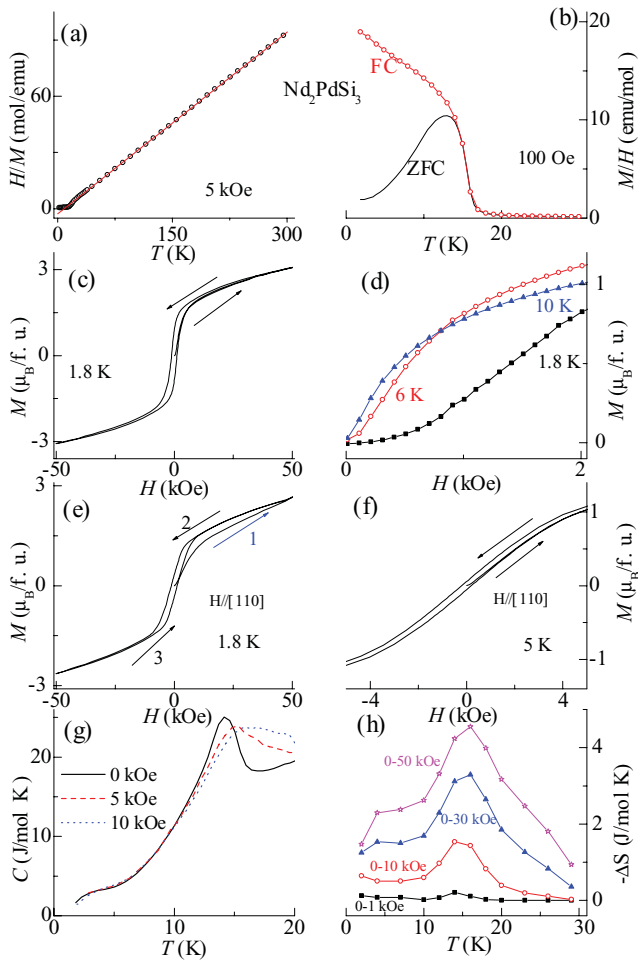


FIG. 2. (Color online) For polycrystalline  $\text{Nd}_2\text{PdSi}_3$ , (a) temperature dependence of inverse susceptibility, with the line through the data points showing the Curie-Weiss fit to the susceptibility; (b) temperature dependence (1.8–30 K) of magnetization divided by magnetic field for ZFC and FC conditions; (c) magnetic hysteresis behavior at 1.8 K; and (d) isothermal magnetization behavior at different temperatures below  $H \leq 2$  kOe. For a single crystalline sample, magnetic hysteresis behavior (data taken in the range 50 to  $-50$  kOe) is shown at (e) 1.8 K and (f) 5 K for  $H//[110]$ . (g) Heat capacity as a function of temperature in the presence of different magnetic fields. (h) Isothermal entropy change ( $\Delta S$ ) as a function of temperature for  $H \leq 50$  kOe for the polycrystal. Unless stated, the lines through the data points serve as visual guides.

suppressed [Fig. 2(d)]. We would naively expect that this step arises from anisotropic coercive FM. However, such flatness can be observed if AFM correlations are present in the virgin state, undergoing metamagnetic transition with increasing field. Therefore, it is not easy to distinguish between these two possibilities. However, a well-known signature of a disorder-broadened first-order transition (as a function of  $H$ ) is that the virgin state tends to lie outside the envelope curve (in the plot of  $M$  versus  $H$ ). A careful look at the inset of Fig. 6(b) in Ref. 21 suggests that, at 2.5 K, the virgin curve beyond the flat region for  $H//[001]$  superimposes over the increasing leg of the envelope curve, which is not typical of a FM loop. We obtained a single crystal from the authors of Ref. 21 and measured  $M(H)$  at 1.8 and 5 K for  $H//[110]$  [Fig. 2(e) and

2(f)]. We found that the virgin curve [marked by path 1 in the Fig. 2(e)] clearly lies outside the envelope curve when the magnetic field is applied along a basal plane at 1.8 K. The virgin curve tends to lie inside the envelope curve at 5 K. On the basis of these observations, we infer that the low-field step in  $M(H)$  well below  $T_o$  is metamagnetic in origin, indicating the existence of an AFM component.

We now discuss the heat capacity behavior of such a complex system. From Fig. 2(g), it is clear that  $C$  shows a peak just below  $T_o$ , and the peak temperature is seen to increase as the magnetic field is increased. This was confirmed by magnetization data, measured in the presence of various magnetic fields (not shown here). Such a feature is characteristic of FM systems. There is a weak drop below 4 K, which could be attributed to the onset of the AFM anomaly discussed earlier. The temperature response of isothermal entropy change [ $\Delta S$  defined as  $S(H) - S(0)$ ] is shown in Fig. 2(h). These  $\Delta S(T)$  curves were obtained from  $M(H)$  isotherms measured at different temperatures (under the ZFC condition after cooling the sample from 50 K) employing the Maxwell equation. Generally, for a FM system  $-\Delta S$  is expected to show a “positive” peak at  $T_o$  due to the loss of spin disorder, while for an AFM a negative peak is observed.<sup>24</sup> The observation of the positive peak around  $T_o$  [Fig. 2(h)] is consistent with a paramagnetic-FM transition.

The temperature dependence of  $\rho$  measured is shown in the inset of Fig. 3. A sharp change of slope is observed around  $T_o$ , which is smeared by the application of a magnetic field. The magnetoresistance [ $\text{MR} = \{\rho(H) - \rho(0)\}/\rho(0)$ ] (Fig. 3) shows interesting features. The sign of MR at 1.8 K is distinctly negative, with a small magnitude for a wide range of magnetic fields, and it becomes positive at a higher field, resulting in a minimum in the plots of  $\text{MR}(H)$  at 15 kOe. The observed positive sign of MR at higher fields is generally uncharacteristic of FM, but this could arise from the AFM component, as proposed earlier. However, as the temperature is increased, the  $\text{MR}(H)$  curve lies in the negative quadrant for the entire field range of the measurement. MR varies nearly as  $H^{2/3}$ , known for FM systems.<sup>25</sup>

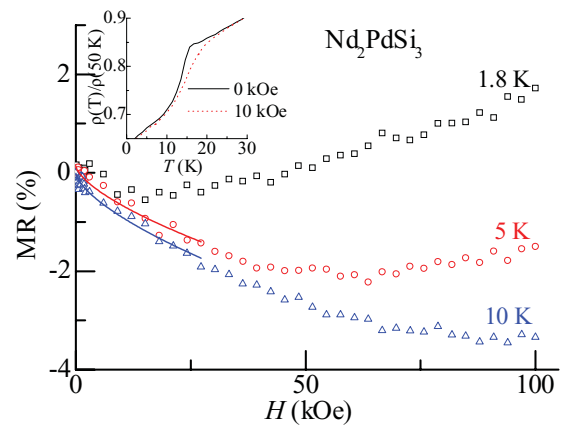


FIG. 3. (Color online) MR as a function of an external magnetic field at selected temperatures. The continuous lines through 5 and 10 K data are drawn to show that MR varies as  $H^{2/3}$  at low fields. Inset: Electrical resistivity  $\rho$  as a function of temperature (1.8–30 K).

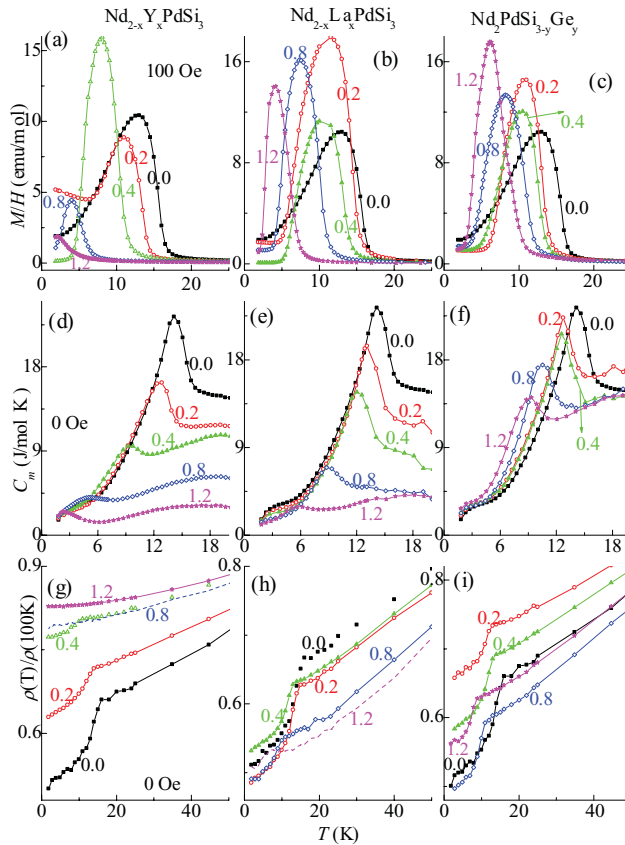


FIG. 4. (Color online) (a)–(c) Temperature dependence (1.8–30 K) of magnetization divided by magnetic field for  $\text{Nd}_{2-x}(\text{Y}, \text{La})_x\text{PdSi}_{3-y}\text{Ge}_y$  ( $x, y = 0.2, 0.4, 0.8$ , and  $1.2$ ) for the ZFC condition of the specimen. (d)–(f) Magnetic specific heat as a function of temperature in the zero field. (g)–(i) Normalized electrical resistivity as a function of temperature in the zero field for all compounds.

This study thus clearly establishes that this compound initially undergoes FM ordering, confirming that this is unique among other members of the  $\text{R}_2\text{PdSi}_3$  series, apart from other low-temperature anomalies. Clearly, the origin of the magnetism of this compound is quite complex.

### B. $4f$ hybridization in doped $\text{Nd}_2\text{PdSi}_3$

Now we focus on the modification of the magnetic properties of the title compound, based on substitutions at the Nd site and at the Si site, viz., on the series  $\text{Nd}_{2-x}(\text{Y}, \text{La})_x\text{PdSi}_{3-y}\text{Ge}_y$  ( $x, y = 0.2, 0.4, 0.8$ , and  $1.2$ ). The lattice parameters tabulated in Table I reveal that for the Y series the lattice constants  $a$  and  $c$  decrease with  $x$ , resulting in a decrease in unit cell volume ( $V$ ), whereas for the La series both increase, leading to an increase in  $V$ . However, for the Ge series  $a$  increases but  $c$  decreases, resulting in an increase in  $V$ .

Figures 4(a)–4(c) shows the temperature-dependent magnetization measured in the presence of a magnetic field of 100 Oe for all alloys. It is clear that  $T_o$  (obtained from the peak of  $d(M/H)/dT$  and tabulated in Table I) is suppressed for all doped compounds. For the Y series,  $T_o$  is suppressed down to 2.9 K for the extreme composition ( $x = 1.2$ ), while for the

La series, it is suppressed to 5.9 K only for the same level of doping. While the suppression of  $T_o$  is a natural consequence of dilution of the magnetic sublattice, the difference in the magnitudes of suppression merits attention. Interestingly, for the Ge series, without disturbing Nd sublattice, a suppression of  $T_o$  (to 7.5 K for  $y = 1.2$ ) is noted even for a marginal increase in volume. This experimentally determined value of the effective moment obtained from the high-temperature Curie-Weiss region is essentially  $\sim 3.5\mu_B/\text{Nd}^{3+}$ , which is in accordance with the free  $\text{Nd}^{3+}$  value.

To gain support for these trends in  $T_o$ , heat capacity and electrical resistivity as a function of temperature were measured for all compounds. The magnetic part of  $C$  ( $C_m$ ) was obtained by subtracting the lattice part, with  $\text{Y}_2\text{PdSi}_3$  and  $\text{La}_2\text{PdSi}_3$  as the reference for lattice contribution for the respective series, employing a procedure given in Ref. 26. The trend observed in  $T_o$ , inferred from magnetization, is also reflected in the  $C$  of all series [Figs. 4(d)–4(f)]. The temperature-dependent normalized resistivity  $\rho(T)$  for all members of the series is shown in Figs. 4(g)–4(i). We plotted normalized resistivity, because the absolute values are not reliable due to microcracks in the specimens. A change of slope in the curve is observed for all members near  $T_o$  (also obtained from the peak of  $d^2\rho/dT^2$  versus  $T$  plots, not shown here). There is a good agreement in the trends of  $T_o$  (within an error of  $\pm 1$  K) obtained from  $M$ ,  $C$ , and  $\rho$  measurements.

It is obvious from the preceding data that, though the trend in the unit cell volume variation is different for the three series, there is a suppression of  $T_o$  in all cases. The magnitude of suppression is different among the three solid solutions. To quantitatively address these variations, the change in  $T_o$  (i.e.,  $\Delta T_o$ ) normalized to the Nd concentration is plotted in Fig. 5(a) as a function of the change in unit cell volume ( $\Delta V$ ) with respect to the parent compound. We first focus on the Y and La substitutions, both of which dilute the Nd sublattice. For a given  $\Delta V$ , the change  $\Delta T_o$  is negligible and nearly constant in the La series, which is consistent with expectations based on indirect exchange interaction. Interestingly, for the Y series, significant suppression of  $T_o$  is observed. This suppression in the Y series compared to that in the La series points to strong  $4f(\text{Nd})$  hybridization with the valence electrons of neighboring ions. Since the substitution of Ge for Si results in an expansion of volume, just based on volume arguments alone, an enhancement in  $\Delta T_o$  is expected on the basis of extrapolation of  $\Delta V$  dependence observed in the Y series, in contrast to the present observations. In addition, for a given  $\Delta V$ , the degree of suppression of  $T_o$  for Ge is much more than that for the Y series, emphasizing the role of  $4f$  ligand hybridization. Since we consider  $\Delta T_o$  to be a measure of the variation in  $4f$  hybridization, then hybridization is stronger for Ge substitution than for Y substitution.

The conclusion that ligand hybridization, rather than volume change, controls variations in magnetic behavior is endorsed by data obtained from high-pressure studies. In Fig. 5(b), the temperature dependencies of magnetization measured in a field of 100 Oe for various values of external pressure in the vicinity of magnetic transition are shown.  $T_o$  remains essentially unchanged up to a pressure of 10 kbar. To make a comparison with the variations in the solid solutions, it is desirable to know the bulk modulus, which is not available

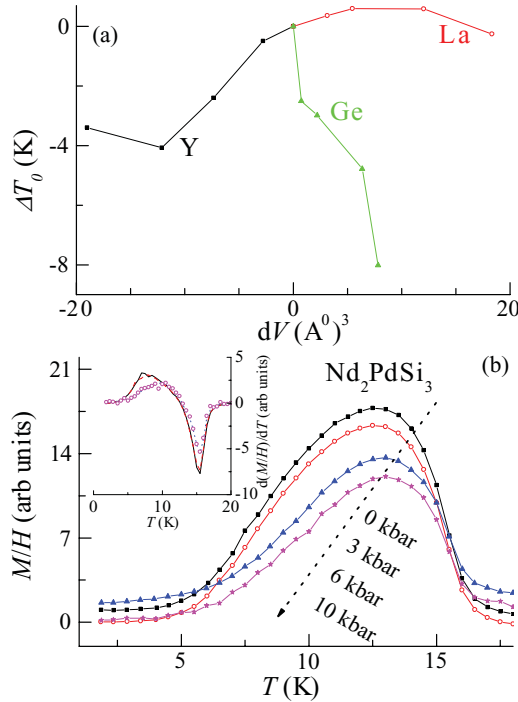


FIG. 5. (Color online) (a) Change  $\Delta T_o$  in magnetic ordering temperature  $T_o$  normalized to the Nd concentration plotted as a function of change in unit cell volume with respect to the parent compound for the compounds in the series  $\text{Nd}_{2-x}(\text{Y, La})_x\text{PdSi}_{3-y}\text{Ge}_y$  ( $x, y = 0.2, 0.4, 0.8, \text{ and } 1.2$ ). (b) Magnetization divided by magnetic field obtained in a field of 100 Oe under the influence of external pressure. The curves are shifted along the y-axis for clarity. Inset: Temperature response of  $d(M/H)/dT$  for all external pressures to show that the magnetic ordering temperature does not vary with pressure.

in the literature. The bulk modulus of Ce compounds falls in the range 60–100 GPa.<sup>27</sup> However, it is not strictly correct to assume that the bulk modulus of Nd compounds are the same as those of Ce systems, considering that 4*f* orbitals in Nd are relatively less hybridized compared to 4*f* orbitals in Ce. In the absence of any knowledge of bulk modulus at present, we use these values for a rough idea, as the preceding bulk modulus range is sufficiently wide. With this caution, for the present alloys, we should see an observable variation of  $T_o$  under pressure. For instance, the pressure exerted by Y substitution for  $x = 0.3$  is of the order of 10 kbar, assuming a bulk modulus of 100 GPa. Clearly,  $V$  variation alone cannot account for the changes in  $T_o$  in solid solutions.

However, there is a contraction along the  $c$ -axis with gradual substitution in the Y and Ge series, whereas in the La series there is an expansion in the  $c$ -direction (Table I). The Pd-Si(Ge) layers (which are sandwiched between Nd layers and stacked in the  $c$ -direction) come closer to Nd ions in the Y and Ge systems, unlike in La-substituted alloys, thereby facilitating 4*f* hybridization with the ligand orbitals in the former cases. Qualitatively, this appears to favor our conclusion of enhancement of 4*f* hybridization in Y- and Ge-based solid solutions. Because the sign of  $\theta_p$  is positive in the  $c$ -direction, as inferred from the data on single crystals,<sup>21</sup> the compression and enhanced hybridization in this direction

may be directly related to depression of FM interaction in these alloys. However, relatively smaller values of  $\Delta T_o$  are observed for the Y series compared to the Ge series for a given  $\Delta c$ , without a quantitative correlation between  $\Delta c$  and  $\Delta T_o$ . This discrepancy can be reconciled by proposing that, in the Y series, the changes induced by the suppression of the  $a$ -parameter have a counterbalancing effect on  $\Delta T_o$ .

In the scenario just discussed, with respect to the differences in 4*f* hybridization in the solid solutions, it is of interest to compare AC- $\chi$  behavior. The real part of AC- $\chi$  at different frequencies is plotted as a function of temperature for the parent compound and the end members in Fig. 6. AC- $\chi$  is frequency dependent below  $T_o$  for all compositions, but the magnitude of the shift in peak temperature (e.g., for a variation of frequency from 1.3 to 931 Hz) is more prominent for Y- and Ge-substituted samples. The peak shift for the La alloy could not be resolved. These findings signal that an increase in 4*f* hybridization favors glassy features. The shift of the peak temperature with frequency is fitted to the power law (which follows from dynamic scaling theory), which is of the form<sup>28</sup>

$$\tau = \tau^0(T/T_f - 1)^{-z\nu},$$

where,  $\tau^0$  is the microscopic flipping time,  $T_f$  is the glass-freezing temperature,  $\nu$  is the critical exponent that describes the growth of spin correlation length, and  $z$  is the dynamic exponent that describes the slowing of relaxation (Fig. 6 insets). For the Y alloy, the fit yielded  $z\nu = 18 \pm 0.35$ ,  $\tau^0 = 4 \times 10^{-8}$ , and  $T_f = 1.6$  K. For  $\text{Nd}_2\text{PdSi}_{1.8}\text{Ge}_{1.2}$ , the shift

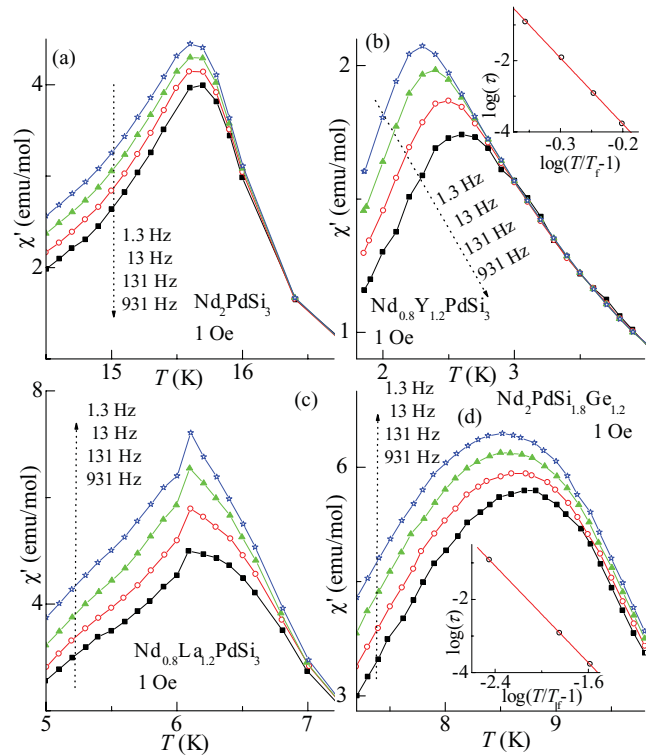


FIG. 6. (Color online) Real part of AC susceptibility at different frequencies plotted as a function of frequency for (a)  $\text{Nd}_2\text{PdSi}_3$ , (b)  $\text{Nd}_{0.8}\text{Y}_{1.2}\text{PdSi}_3$ , (c)  $\text{Nd}_{0.8}\text{La}_{1.2}\text{PdSi}_3$ , and (d)  $\text{Nd}_2\text{PdSi}_{1.8}\text{Ge}_{1.2}$ . Insets show dynamic scaling fit of the peak temperature with the reduced temperature for  $\text{Nd}_{0.8}\text{Y}_{1.2}\text{PdSi}_3$  and  $\text{Nd}_2\text{PdSi}_{1.8}\text{Ge}_{1.2}$ .

in peak temperature when fitted with the power law yields  $z\nu = 3 \pm 0.2$ ,  $\tau^0 = 10^{-9}$ , and  $T_f = 8.5$  K. Characterization of the frequency dependence of  $T_f$  was carried out by relative shift in  $T_f$  per decade of frequency, i.e.,  $\delta f = \Delta T_f / T_f \times \Delta \ln \nu$ . Even though the values of  $\delta f$  lie in the range 0.03–0.003, which is similar to that observed for spin glasses,<sup>29</sup> we do not classify these compounds as a spin glass, considering that the features in heat capacity are well defined at the magnetic transition.

#### IV. CONCLUSIONS

The present study establishes that magnetism of  $\text{Nd}_2\text{PdSi}_3$  is unique in the sense that this compound orders ferromagnetically ( $\sim 15.5$  K), unlike other members of this series, in addition to possible onset of AFM correlations at much lower temperatures. We identified a Nd-based compound, in which Nd  $4f$  hybridization apparently plays a major role in magnetism, making it different from other members in this ternary family. This conclusion is based on a comparative investigation

of the solid solutions  $\text{Nd}_{2-x}(\text{Y}, \text{La})_x\text{PdSi}_{3-y}\text{Ge}_y$  ( $x, y = 0.2, 0.4, 0.8, \text{ and } 1.2$ ), as well as high-pressure studies. These studies reveal a strengthening  $4f(\text{Nd})$  hybridization with the valence electrons of other ions in the Y- or Ge-substituted samples. Interestingly, stronger hybridization seems to favor development of glassy features near the magnetic transitions. In short, this work emphasizing the role of Nd  $4f$  hybridization on magnetism adds a new input to the field of strongly correlated electron systems. We believe that such systems could open an exciting avenue to understand heavy-fermion behavior and quantum critical point effects among Nd-based systems, e.g., by extending studies to very high pressures.

#### ACKNOWLEDGEMENT

The authors thank W. Loeser and Y. Xu (Leibnitz-Institute fuer Festkoerper-und Werkstofforschung, Dresden, Germany) for making their single crystals available to us for some magnetization measurements.

\*kmukherjee@tifr.res.in

†sampath@mailhost.tifr.res.in

<sup>1</sup>See, e.g., E. D. Bauer, N. A. Frederick, P.-C. Ho, V. S. Zapf, and M. B. Maple, *Phys. Rev. B* **65**, 100506(R) (2002); A. Yatskar, W. P. Beyermann, R. Movshovich, and P. C. Canfield, *Phys. Rev. Lett.* **77**, 3637 (1996); Y. Aoki, T. Namiki, T. D. Matsuda, K. Abe, H. Sugawara, and H. Sato, *Phys. Rev. B* **65**, 064446 (2002).

<sup>2</sup>R. D. Parks, S. Raaen, M. L. denBoer, Y.-S. Chang, and G. P. Williams, *Phys. Rev. Lett.* **52**, 2176 (1984); G. Kalkowski, E. V. Sampathkumaran, C. Laubschat, M. Domke, and G. Kaindl, *Solid State Comm.* **55**, 977 (1985); Y. Kucherenko, S. L. Molodtsov, A. N. Yaresko, and C. Laubschat, *Phys. Rev. B* **70**, 045105 (2004).

<sup>3</sup>P. A. Kotsanidis and J. K. Yakinthos, *J. Magn. Magn. Mater.* **87**, 199 (1990).

<sup>4</sup>R. Mallik, E. V. Sampathkumaran, M. Strecker, G. Wortmann, P. L. Paulose, and Y. Ueda, *J. Magn. Magn. Mater.* **185**, L135 (1998).

<sup>5</sup>R. Mallik, E. V. Sampathkumaran, M. Strecker, and G. Wortmann, *Europhys. Lett.* **41**, 315 (1998); R. Mallik, E. V. Sampathkumaran, and P. L. Paulose, *Solid State Comm.* **106**, 169 (1998).

<sup>6</sup>S. Majumdar, E. V. Sampathkumaran, D. Eckert, A. Handstein, K.-H. Müller, S. R. Saha, H. Sugawara, and H. Sato, *J. Phys. Condens. Matter* **11**, L329 (1999).

<sup>7</sup>A. Szytula, M. Hofmann, B. Penc, M. Slaski, S. Majumdar, E. V. Sampathkumaran, and A. Zygmunt, *J. Magn. Magn. Mater.* **202**, 365 (1999).

<sup>8</sup>S. R. Saha, H. Sugawara, T. D. Matsuda, H. Sato, R. Mallik, and E. V. Sampathkumaran, *Phys. Rev. B* **60**, 12162 (1999).

<sup>9</sup>S. R. Saha, H. Sugawara, T. D. Matsuda, Y. Aoki, H. Sato, and E. V. Sampathkumaran, *Phys. Rev. B* **62**, 425 (2000).

<sup>10</sup>S. Majumdar, E. V. Sampathkumaran, P. L. Paulose, H. Bitterlich, W. Löser, and G. Behr, *Phys. Rev. B* **62**, 14207 (2000).

<sup>11</sup>S. Majumdar and E. V. Sampathkumaran, *J. Magn. Magn. Mater.* **223**, 247 (2001).

<sup>12</sup>S. Majumdar, H. Bitterlich, G. Behr, W. Löser, P. L. Paulose, and E. V. Sampathkumaran, *Phys. Rev. B* **64**, 012418 (2001).

<sup>13</sup>A. N. Chaika, A. M. Ionov, M. Busse, S. L. Molodtsov, S. Majumdar, G. Behr, E. V. Sampathkumaran, W. Schneider, and C. Laubschat, *Phys. Rev. B* **64**, 125121 (2001).

<sup>14</sup>E. V. Sampathkumaran, H. Bitterlich, K. K. Iyer, W. Löser, and G. Behr, *Phys. Rev. B* **66**, 052409 (2002).

<sup>15</sup>D. X. Li, S. Nimori, Y. Shiokawa, Y. Haga, E. Yamamoto, and Y. Onuki, *Phys. Rev. B* **68**, 012413 (2003).

<sup>16</sup>P. L. Paulose, E. V. Sampathkumaran, H. Bitterlich, G. Behr, and W. Löser, *Phys. Rev. B* **67**, 212401 (2003).

<sup>17</sup>S. Nimori and D. Li, *J. Phys. Soc. Jpn.* **75**, 195 (2006).

<sup>18</sup>D. S. Inosov, D. V. Evtushinsky, A. Koitzsch, V. B. Zabolotnyy, S. V. Borisenko, A. A. Kordyuk, M. Frontzek, M. Loewenhaupt, W. Löser, I. Mazilu, H. Bitterlich, G. Behr, J.-U. Hoffmann, R. Follath, and B. Büchner, *Phys. Rev. Lett.* **102**, 046401 (2009).

<sup>19</sup>M. Frontzek, F. Tang, P. Link, A. Schneidewind, J.-U. Hoffman, J.-M. Mignot, and M. Loewenhaupt, *Phys. Rev. B* **82**, 174401 (2010).

<sup>20</sup>T. Nakano, K. Sengupta, S. Rayapol, M. Hedo, Y. Uwatoko, and E. V. Sampathkumaran, *J. Phys. Condens. Matter* **19**, 326205 (2007).

<sup>21</sup>Y. Xu, W. Loser, F. Tang, C. G. F. Blum, L. Liu, and B. Buchner, *Cryst. Res. Technol.* **46**, 135 (2011).

<sup>22</sup>R. L. Carlin, in *Magnetochemistry*, edited by R. L. Carlin (Springer-Verlag, Berlin, 1986), pp. 146.

<sup>23</sup>S. B. Roy, A. K. Pradhan, P. Chaddah, and E. V. Sampathkumaran, *J. Phys. Condens. Matter* **9**, 2465 (1997).

<sup>24</sup>K. A. Gschneidner Jr., V. K. Pecharsky, and A. Tsokol, *Rep. Prog. Phys.* **68**, 1479 (2005).

<sup>25</sup>J. M. Fournier and E. Gartz, in *Handbook on the Physics and Chemistry of Rare Earths*, edited by K. A. Gschneidner Jr. and L. Eyring (North-Holland, Amsterdam, 1993), Vol. 17, pp. 109.

<sup>26</sup>M. Bouvier, P. Lethuillier, and D. Schmitt, *Phys. Rev. B* **43**, 13137 (1991).

<sup>27</sup>R. S. Kumar, A. L. Cornelius, and J. L. Sarrao, *Phys. Rev. B* **70**, 214526 (2004); G. Oomi, Y. Uwatoko, E. V. Sampathkumaran, and M. Ishikawa, *Phys. B* **223&224**, 307 (1996).

<sup>28</sup>P. C. Hohenberg and B. I. Halperin, *Rev. Mod. Phys.* **49**, 435 (1977).

<sup>29</sup>J. A. Mydosh, *J. Magn. Magn. Matter* **157**, 606 (1996); J. Souletie and J. L. Tholence, *Phys. Rev. B* **32**, 516 (1985); C. A. M. Mulder, A. J. van Duynveldt, and J. A. Mydosh, *ibid.* **25**, 515 (1982); and references therein.